

Epitope mapping of a new anti-Tn antibody detecting gastric cancer cells

Nina Persson², Nicolai Stuhr-Hansen², Christian Risinger², Stefan Mereiter^{3,4,5}, António Polónia^{3,4,6}, Karol Polom⁷, András Kovács^{2,8}, Franco Roviello⁷, Celso A Reis^{3,4,5,9}, Charlotte Welinder^{10,11}, Lena Danielsson⁸, Bo Jansson^{10,12}, and Ola Blixt^{1,2,12}

² Chemical Glyco-Biology Laboratory, Department of Chemistry, University of Copenhagen, 2100 Copenhagen, Denmark,

³ I3S—Instituto de Investigação e Inovação em Saúde, University of Porto, 4200-135 Porto, Portugal,

⁴ Institute of Molecular Pathology and Immunology of the University of Porto—IPATIMUP, 4200-135 Porto, Portugal,

⁵ Institute of Biomedical Sciences of Abel Salazar—ICBAS, University of Porto, 4050-343 Porto, Portugal,

⁶ Department of Pathology, IPATIMUP Diagnostics, IPATIMUP, University of Porto, 4200-135 Porto, Portugal,

⁷ Unit of Surgical Oncology, Department of Surgical Medical Science and Neurosciences, University of Siena, Siena 53100, Italy,

⁸ Division of Clinical Chemistry and Pharmacology, Department of Laboratory Medicine, Lund University, 221 85 Lund, Sweden,

⁹ Medical Faculty, University of Porto, 4200-319 Porto, Portugal,

¹⁰ Division of Oncology and Pathology, Department of Clinical Sciences Lund, Lund University, 221 85 Lund, Sweden, and

¹¹ Centre of Excellence in Biological and Medical Mass Spectrometry (CEBMMS), Biomedical Centre D13, Lund University, 221 84 Lund, Sweden

¹ To whom correspondence should be addressed: Tel: +46-761486838; e-mail: olablixt@chem.ku.dk

¹² These authors contributed equally to the work.

Originally published in *Glycobiology*. 2017 Jul 1;27(7):635-645. doi: 10.1093/glycob/cwx033

Keywords: gastric cancer, glycosylation, N-acetylgalactosamine (GalNAc), scFv, solid-phase peptide synthesis, Tn-antigen

Issue Section: Chemical Biology

INSTITUTO
DE INVESTIGAÇÃO
E INOVAÇÃO
EM SAÚDE
UNIVERSIDADE
DO PORTO

Rua Alfredo Allen, 208
4200-135 Porto
Portugal
+351 220 408 800
info@i3s.up.pt
www.i3s.up.pt

Version: Postprint (identical content as published paper) This is a self-archived document from i3S – Instituto de Investigação e Inovação em Saúde in the University of Porto Open Repository For Open Access to more of our publications, please visit <http://repositorio-aberto.up.pt/>

ABSTRACT

Here, we introduce a novel scFv antibody, G2-D11, specific for two adjacent Tn-antigens (GalNAc-Ser/Thr) binding equally to three dimeric forms of the epitope, Ser-Thr, Thr-Thr and Thr-Ser. Compared to other anti-Tn reagents, the binding of G2-D11 is minimally influenced by the peptide structure, which indicates a high degree of carbohydrate epitope dominance and a low influence from the protein backbone. With a high affinity ($K_{Dapp} = 1.3 \times 10^{-8}$ M) and no cross-reactivity to either sialyl-Tn epitope or blood group A antigens, scFv G2-D11 is an excellent candidate for a well-defined anti-Tn-antigen reagent. Detailed immunohistochemical evaluation of tissue sections from a cohort of 80 patients with gastric carcinoma showed in all cases positive tumor cells. The observed staining was localized to the cytoplasm and in some cases to the membrane, whereas the surrounding tissue was completely negative demonstrating the usefulness of the novel Tn-antigen binding antibody.

INTRODUCTION

A common *O*-linked glycosylation with *N*-acetylgalactosamine (GalNAc) occurs at serine (Ser) or threonine (Thr) residues of glycoproteins and is known as the Tn-antigen. The Tn-antigen is the precursor for extended *O*-glycans and is shielded by the elongated structures in healthy and benign tissues. Cancer cells often have an altered glycosylation biosynthesis leading to the expression of aberrant carbohydrate structures on the cell surface (Gill et al. 2010; Pinho and Reis 2015). These modified glycans play a role in intercellular recognition and adhesion, as well as in tumor invasion and metastasis (Pinho and Reis 2015). Truncated glycan structures, like the Tn-antigen, have been associated with a variety of human carcinomas, e.g., colon, breast, lung, bladder, cervix, ovarian, stomach and prostate cancer (Hamada et al. 1993; Desai 2000; Oshikiri et al. 2006). The Tn-antigen is present on many different proteins. Different mucins in carcinomas carry a high density of Tn-antigens (Ju et al. 2011) and leukemic cells have been found to carry Tn-antigen on CD43 (sialophorin) (Nakada et al. 1991). The IgA1 immunoglobulin, with a hinge region that can carry the Tn-antigen, is believed to be involved in autoimmune disease (Tomana et al. 1999) and has also been associated with breast cancer (Welinder et al. 2013). These tumor-associated antigens, which are ectopically expressed in cancer cells, could be used as potential targets for both diagnosis and therapy (Avichezer et al. 1997; Springer 1997; Yu 2007; Welinder et al. 2011; Posey et al. 2016).

A number of antibodies with different specificities for the Tn-antigen have been generated (Takahashi et al. 1988; Numata et al. 1990; Pancino et al. 1990; Avichezer et al. 1997; Reis et al. 1998; Ando et al. 2008). Many of these Tn-specific monoclonal antibodies (mAbs) recognized clusters composed of two or three consecutive glycosylated Ser/Thr residues. In some cases, the antibody is dependent on the peptide sequence of the glycoprotein and thereby recognizing a glycopeptide-specific epitope (Reis et al. 1998; Brooks et al. 2010; Blixt et al. 2012b). Many different anti-Tn antibodies have been used for immunohistochemistry (IHC) evaluation (Ohshio et al. 1995; Zhang et al. 1998; Welinder et al. 2011) with varying outcome, regarding both the intensity and the frequency of Tn-expression. This was clearly illustrated in a prostate cancer study, where the IHC results of four different Tn-binding reagents were compared with carbohydrate microarray analysis (Li et al. 2009). The fine specificity was shown to differ between the Tn-binding reagents

with a preference for clustered Tn-antigens, but with reagents also recognizing the single Tn-antigen or demonstrating cross-reactivity to blood group A (Li et al. 2009).

The complexity of the Tn-antigen increases with the possibility of *O*-GalNAc to be associated with either serine or threonine and with the mono- or multimeric formations on proteins. These details will influence the flexibility and overall global shape of the glycoprotein and the binding of lectins (Madariaga et al. 2014, 2015).

The evaluation of antibody specificity is an essential part in the development of antibodies to be used for diagnosis or therapy. In this study, we have analyzed the fine specificity of a new single-chain fragment variable (scFv) antibody, G2-D11, with two glycopeptide libraries, one based on trimer and one on 20-mer peptides, presenting GalNAc-Ser and GalNAc-Thr in different combinations. In a cohort of gastric carcinoma, the staining of the cytoplasm and, in some cases, the membrane was observed with the G2-D11. The different staining pattern between gastric carcinoma with cytoplasmic and membrane staining and adjacent mucosa with perinuclear staining, indicate that G2-D11 could be used as a tool for diagnostic and therapeutic purpose.

RESULTS

Tn-peptide microarray library

G2-D11 is one of the Tn-antigen binding scFvs obtained from an antibody phage library generated from mice immunized with glycopeptides as previously described (Persson et al. 2016). To evaluate the specificity of G2-D11, a large synthetic glycopeptide library was constructed and printed on microarray glass slides. The library contained trimer amino acid combinations of GalNAc-Ser (S*) and GalNAc-Thr (T*) flanked by different combinations of amino acids (X). The library was organized into five groups, depending on the position of the GalNAc on either Ser or Thr residues. Group 1 consisted of two GalNAc-Thr residues at the C-terminal end. Group 2 consisted of two GalNAc-Thr residues at the N-terminal, and Group 3 started with one amino acid without glycosylation, followed by one GalNAc-Thr and one GalNAc-Ser residue. Group 4 consisted of an N-terminal GalNAc-Ser and a GalNAc-Thr residue followed by a C-terminal amino acid, and Group 5 had a nonglycosylated amino acid on both sides of a single GalNAc-Thr residue (Figure 1). The *Vicia villosa* lectin (VVL) binds both mono- and multimeric forms of the Tn-antigen (Osinaga et al. 2000; Wu 2004) and is used as a control for surface immobilization of all synthetic Tn-glycopeptides (Figure 2).

Specificity analysis

Previously published mouse monoclonal Tn antibodies, GOD3-2C4 (Welinder et al. 2013), MLS128 (Ohshio et al. 1995) and the scFv version of GOD3-2C4 (sH1), were compared with G2-D11 for binding to the trimer glycopeptide library (Figure 2). Both G2-D11 and GOD3-2C4 bound to two adjacent Tn-antigens flanked by most amino acid combinations. In Group 1, which included two adjacent GalNAc-Thr residues, the presence of proline (Pro) and glutamic acid (Glu) residues reduced the binding of G2-D11 (Figure 2A, circled in red). MLS128 was more sensitive to the amino acid present next to the two adjacent GalNAc-Thr residues. A binding similar to the ones seen with G2-D11 and GOD3-2C4 could only be observed for the amino acids cysteine (Cys), lysine (Lys), arginine (Arg) and tryptophan (Trp) (Figure 2A, circled in red).

When changing the position of the amino acid residues to the C-terminal side of the two adjacent GalNAc-Thr residues (represented by Group 2), G2-D11 and GOD3-2C4 still bound to the most amino acid combinations, but both were affected by the amino acids leucine (Leu) and glycine (Gly) and additionally valine (Val), and isoleucine (Ile) for GOD3-2C4 (Figure 2B, circled in red). Most of the amino acid combinations reduced the binding of MLS128, showing only elevated binding for Glu (Figure 2B, circled in red).

When one of the GalNAc-Thr residues was exchanged with a GalNAc-Ser residue in Group 3, the G2-D11 and GOD3-2C4 still bound to most of the combinations, but neighboring amino acids, particularly Glu and glutamine (Gln) prevented the binding of G2-D11 (Figure 2C, circled in red). No binding could be seen with MLS128 with the exception of amino acid Trp (Figure 2C, circled in red). In Group 4, G2-D11 bound to all amino acid combinations while the binding of GOD3-2C4 was reduced by Glu (Figure 2D, circled in red). With the GalNAc-Ser/GalNAc-Thr in Group 4, MLS128 showed slightly elevated signals compared to GalNAc-Thr/GalNAc-Ser in Group 3 and bound only weakly to Arg (Figure 2D, circled in red). In Group 5, different combinations with single GalNAc-Thr were tested. Only GOD3-2C4 and G2-D11 showed some binding events (Figure 2E and F, circled in red) in the representative graphs of different monomeric Tn-antigen combinations. G2-D11 bound to a few combinations containing Trp, tyrosine (Tyr) and alanine (Ala) while GOD3-2C4 bound to many combinations with Trp and to some with Tyr and phenylalanine (Phe). The sH1 showed low binding to all of the Group 1–5a, b (Figure 2).

A second glycopeptide library was used to evaluate the specificity based on a titration of the antibodies and consisted of tetra- and 20-mer glycopeptides, 20-mers of mucin-1 (Muc1) with sialyl-Tn-antigen (STn-antigen) and blood group A antigen (Table I). The library was printed on a microarray slide and evaluated using G2-D11, sH1, GOD3-2C4 and MLS128 at different concentrations (Figure 3A). The anti-STn-antigen antibodies, B72.3 and CC49, were used as positive controls for STn-antigen on Muc1 (peptide 24 and 25; Figure 3B). The previous microarray result, where G2-D11 bound to two adjacent GalNAc-epitopes, was confirmed (Table I, peptides 1, 2, 9, 12, 13, 14, 18, 19 and 20; Figure 3A). At higher concentrations, the sH1 scFv bound to two adjacent GalNAc-epitopes in combination S*T* (peptide 9, 18 and 19), but not to any of the single GalNAc epitopes (Figure 3A). The GOD3-2C4 also bound a single GalNAc-Ser residue, besides binding two or three adjacent GalNAc epitopes (peptides 3, 6, 7, 10 and 21), but also demonstrated cross-reactivity with the blood group A antigen (peptide 26) (Figure 3A). Unlike GOD3-2C4, MLS128 did not bind single GalNAc epitopes and preferred two or three adjacent GalNAc-epitopes on 20-mer peptides to tetramer epitopes (peptides 1, 9, 12, 18 and 19) (Figure 3A). None of the antibodies G2-D11, sH1, GOD3-2C4 or MLS128 were cross-reactive with the STn-antigen (Figure 3A). Both anti-STn antibodies, B72.3 and CC49, showed cross-reactivity to the Tn-antigen (peptides 1, 9, 18 and 19), but clearly preferred the STn-epitope (peptide 24 and 25) at these assay conditions (Figure 3B). The Tn-binding antibodies were also analyzed for binding to two adjacent GalNAc-serines on the CD44-peptide WVNRRGESSRKAYDHNSPY (Supplementary data, Figure S1). Only G2-D11 and GOD3-2C4 bound to the glycopeptide while sH1 and MLS128 were negative. G2-D11 did not bind any other related carbohydrate structures (e.g., GalNAc β , GalNAc α 1-3GalNAc α , GalNAc α 1-3(Fuc α 1-2)Gal β 1-3GlcNAc β , GlcNAc α , GlcNAc β) tested on a large carbohydrate microarray chip and no binding to other carbohydrate or single GalNAc epitope was observed (data not shown; a list of the tested carbohydrates is presented in Supplementary data, Table S1). GOD3-2C4 demonstrated cross-reactivity to GalNAc α 1-3Gal β -, Core 5, Core 6, Gal β 1-4GlcNAc β 1-6GalNAc α - and GalNAc α 1-3GalNAc(fur) β - (data not shown).

Analysis of binding kinetics

The analysis of binding kinetics of G2-D11 to two adjacent GalNAc on a 20-mer peptide (Table I, peptide 9) was made with bio-layer interferometry (BLI). Two different approaches were tested to measure the on- and off-rates to calculate a dissociation constant. In the first approach, the biotinylated target peptide was immobilized on streptavidin sensor tips and in the second approach, the G2-D11 and sH1 were immobilized on nickel-nitrilotriacetic acid (Ni-NTA) sensor tips through their histidine (His)-tags. Using either of the two methods, the G2-D11 dissociation constant was determined to be in the nanomolar range (Table II, complete sensogram in [Supplementary data, Figure S2](#)). GOD3-2C4 had a dissociation constant in the same range as G2-D11, but was only analyzed with immobilized glycopeptide as it lacks the His-tag. The sH1 generated a weak signal that did not fit the 1:1 Langmuir model and no conclusion could be drawn from the analysis by either methods.

Immunofluorescence staining of MKN45 cells

We used the gastric carcinoma cell line MKN45, stably transfected with *ST6GALNAC1*, as a model to evaluate antibody binding in a relevant biological context. This cell line has previously been described to overexpress STn-antigen compared to the mock control cell line transfected with an empty vector (Marcos et al. 2004). Fixed mock and *ST6GALNAC1*transfected MKN45 cells were incubated with G2-D11, sH1 or GOD3-2C4. Both GOD3-2C4 and G2-D11 showed punctuated intracellular staining in the mock transfected cells and sH1 showed a much weaker staining (Figure 4A). GOD3-2C4 showed increased cytoplasmic staining with indications of membranous staining in the *ST6GALNAC1*transfected cells in contrast to G2-D11, which maintained the punctuated intracellular staining pattern (Figure 4A). The *ST6GALNAC1*transfected cells were treated with neuraminidase which significantly reduced binding of the anti-STn antibody, B73.2 (Figure 4B). The staining of the Tn-antigen with G2-D11 was seen to change from the punctuated intracellular staining in the nonneuraminidase-treated cells to increased diffuse cytoplasmic staining with indications of membranous staining in the neuraminidase-treated cells (Figure 4B).

IHC analysis

The staining of G2-D11 was compared to the staining of GOD3-2C4 and sH1 on a series of human gastric carcinoma using IHC where 1E3 was used as a positive control (Figure 5) (Blixt et al. 2012a). In intestinal metaplasia, a premalignant condition, the G2-D11 stained specifically the perinuclear region correlating with Golgi apparatus of the cells. The GOD3-2C4 also stained the vacuoles of goblet cells in intestinal metaplasia. These vacuoles are rich in mature mucins, mostly mucin-2 carrying STn-antigen (Ferreira et al. 2006). The staining of carcinoma cells with G2-D11 and GOD3-2C4 was not restricted only to the perinuclear compartments but was found in the cytoplasm, in the cellular membrane and also on secreted glycoproteins in the mucin lakes. In addition, G2-D11 stained larger tumor areas and with higher intensity than GOD3-2C4. The staining with sH1 was very weak in all parts of the tissue. All the tested antibodies showed staining exclusively in epithelial and carcinoma cells.

Formalin fixed paraffin embedded tissue sections from a cohort of 80 patients with gastric carcinoma were all stained positive in IHC with G2-D11. The antibody gave a clear image with low background and intense tumor staining (Figure 6). Frequency and intensity of staining in tumor and

adjacent mucosa are presented in Table III and Figure 6. The staining was mainly localized to perinuclear in the adjacent mucosa (73%, Figure 6A) and in some cases a cytoplasmic staining could also be seen (Figure 6B). In all cases, tumor cells showed mainly cytoplasmic staining (Table III, Figure 6C and D) and 24 cases had more than 75% of the tumor area stained with medium (++) to high intensity (+++). A clear enriched staining at the cancer cell membrane could be seen in seven cases (Figure 6E and F). In 22 of the 25 cases that presented mucin lakes within the tumor area, the mucin lakes were stained with G2-D11 (Figure 6G). This indicates a frequent ectopic expression of the Tn epitope in the secretome and a good sensitivity of G2-D11 to detect the mucin lakes.

DISCUSSION

In this study, we have performed an extended analysis of the epitope defined by a new anti-Tn-antigen antibody, G2-D11, using different microarray analysis, affinity measuring as well as immunofluorescence staining on gastric cancer cell lines and IHC on tissues from patients with gastric carcinoma.

The G2-D11 antibody bound specifically to two adjacent Tn-antigens independently of their different positions on Ser and Thr residues, and with low influence from surrounding amino acids (Figures 2 and 3). It bound weakly to single GalNAc-Ser but not to STn-antigen. In contrast to GOD3-2C4 and MLS128, G2-D11 did not show any cross-reactivity to the blood group A antigen.

Additionally, to the specificity evaluation of G2-D11, an extensive binding kinetics analysis was performed. When using, techniques involving immobilization, the interacting part in solution must be of monovalent nature to avoid artifacts due to the multivalent binding. The most common way of analyzing the binding constant involves immobilization of the antigen but when analyzing bivalent or dimeric antibodies there is a risk of measuring avidity instead of affinity. For kinetic binding analysis, two different setups were used in this study. The first involved immobilization of biotinylated antigen on streptavidin biosensors and in the second, the histidine-tag of scFv was used for immobilization on Ni-NTA biosensors. The binding kinetics data for G2-D11 resulted in similar on- and off-rates (reflecting how fast the antibody binds to or dissociate from the target) for both setups, indicating that the analysis was not affected by multimerization and an apparent K_D value in the nanomolar range (10^{-8}) could be calculated (Table II). The G2-D11 demonstrated an affinity constant in the same range as IgG, GOD3-2C4 and MLS128, and the IgM 83D4 (Osinaga et al. 2000) and a 10- to 100-fold higher affinity constant compared to previously described Tn-antigen binding scFv, 4E10, 4G2 and scFv of MLS128, which show K_D values in the micromolar range (10^{-6}) (Sakai et al. 2010; Yuasa et al. 2012). The binding kinetics data for sH1 could not be evaluated since the sensogram differed from the 1:1 curve fitting model. Since sH1 is the scFv version of IgG1 GOD3-2C4, it is expected to bind the same antigen but with lower affinity. Both the BLI analysis and the microarray analysis indicate that sH1 binds to the target antigen but with a weak interaction. This could be due the monovalent binding of scFv compared to the multivalent binding of GOD3-2C4 or to partly changed structure of scFv upon expression compared to GOD3-2C4.

A diffuse cytoplasmic and membranous staining pattern of MKN45 cells transfected with ST6GALNAC1 have previously been seen by two Tn-binding antibodies, 1E3 and HB-Tn (Pinho et al. 2007). The punctuated cytoplasmic staining of mock transfected MKN45 cells was observed for both G2-D11 and GOD3-2C4 (Figure 4A), similar to the staining of Golgi seen by anti-Tn antibody on

HeLa cells after EGF treatment (Gill et al. 2010). The *ST6GALNAC1* transfected cells showed a more diffuse cytoplasmic staining by GOD3-2C4, as compared to mock transfected cells (Figure 4A). In contrast, the subcellular localization of G2-D11 binding was not affected by the overexpression of *ST6GALNAC1*. The Tn-antigen specificity of G2-D11 was verified when the staining of *ST6GALNAC1* transfected MKN45 cells was increased and changed to diffuse cytoplasmic staining with indications of membranous staining after neuraminidase treatment. This resembles the B72.3 staining of nontreated cells and correlates with the change from STn- to Tn-antigen. The B72.3 staining of *ST6GALNAC1* transfected cells was reduced with neuraminidase demonstrating that B72.3 prefers the STn-epitope. This binding is probably due to higher affinity for STn-antigen than Tn-antigen as the microarray analysis resulted in a binding to Tn-antigen at high concentrations.

Previously it was shown that different Tn-antigen binding antibodies stain prostate cancer (Li et al. 2009), colon and breast cancer (Mazal et al. 2013) with different intensity and frequency. This is probably due to their differences in fine specificity, affinity or cross-reactivity. In this study, tissues from gastric carcinoma were used for comparing the staining pattern of G2-D11 with GOD3-2C4, sH1 and 1E3 (Figure 5). Both major histological subtypes, intestinal and diffuse, were included in the comparison which commonly also included adjacent gastric mucosa and adjacent premalignant lesions such as dysplasia, hyperplasia and intestinal metaplasia. Briefly, all antibodies, except sH1, stained perinuclear adjacent premalignant lesions and normal adjacent gastric mucosa. Perinuclear staining has been reported with MLS128 in normal columnar epithelium (Ohshio et al. 1995). The perinuclear stain, seen in Figure 5A and B, is believed to be associated mainly with Golgi, a place for the majority of O-glycosylation. In cancer, altered expression of glycosyltransferases and relocation of transferases from Golgi into the ER lead to change in the pattern of O-glycosylation and also correlates with increased migration and a metastatic behavior of the tumor. The spread of staining in IHC to cytoplasm and plasma membrane indicate an increase in the presence of different proteins carrying the bis-Tn epitope. GOD3-2C4 stained the vacuoles of goblet cells in intestinal metaplasia, indicating that the goblet cells, in addition to high expression of STn-antigen (Ferreira et al. 2006; Conze et al. 2009), may also express the Tn epitope. The difference in staining pattern could relate to the specificity of the antibody, where G2-D11 bind to all combinations of two adjacent Tn-antigens regardless of peptide backbone and GOD3-2C4 recognizes additional epitopes such as single Tn-antigen and blood group A antigen.

Staining of tissue sections from 80 cases of gastric carcinoma confirms the preliminary results from the comparison of the Tn-antibodies (Figure 5), showing perinuclear staining of adjacent mucosa. Moreover, we confirmed in all carcinoma cases the ectopic diffuse cytoplasmic staining (Table III) which has also been reported for MLS128 in stomach adenocarcinoma (Ohshio et al. 1995). The G2-D11 has increased sensitivity in gastric carcinomas to detect Tn-antigen compared to GOD3-2C4 or other anti-Tn mAbs (Figure 5). The detection of secreted proteins as demonstrated in the mucin lakes (Table III and Figure 6) and the absence of staining of secretory vacuoles in premalignant lesions (Figure 5), render G2-D11 as a candidate for biomarker detection to be used in IHC.

In conclusion, G2-D11 is a high affinity antibody specific for the bis-Tn epitope (two adjacent O-GalNAc) independent of the carrier protein. The antibody's fine specificity results in a clear difference between IHC staining patterns of tumor area and adjacent mucosa. This should make G2-D11 useful as a highly specific reagent for detection of bis-Tn epitope (Tn2) in biological samples.

MATERIALS AND METHODS

Materials

General chemicals were purchased from Sigma-Aldrich (Denmark). The Fmoc (9-fluorenylmethyloxycarbonyl)-protected amino acids, MeOH, *N*-methyl-2-pyrrolidone, *N,N*-dimethylformamide, piperidine, trifluoroacetic acid, *N*-[(1*H*-benzotriazol-1-yl)(dimethylamino)methylene]-*N*-methylmethan-aminium-hexafluoro-phosphate-*N*-oxide, and 1-Hydroxy-7-azabenzotriazole were purchased from Iris Biotech GmbH (Marktredwitz, Germany). *N*- α -Fmoc-*O*- β -(2-acetamido-2-deoxy-3,4,6-tri-*O*-acetyl- β -D-galactopyranosyl)-L-serine (Fmoc-Ser(β -D-GalNAc(Ac)₃)-OH) and *N*- α -Fmoc-*O*- β -(2-acetamido-2-deoxy-3,4,6-tri-*O*-acetyl- β -D-galactopyranosyl)-L-threonine (Fmoc-Thr(β -D-GalNAc(Ac)₃)-OH) were purchased from Sussex Research Laboratories, Inc. (Ontario Canada). Monoclonal antibodies GOD3-2C4 (Welinder et al. 2011), MLS128 binding to Tn-antigen (Cat. No #017-25,891, Wako), B72.3 binding to STn-antigen (Cat. No ab691, abcam) and also used as hybridoma supernatant, and CC49 binding to STn-antigen (Cat. No ab16838, abcam) were used in this study. ScFv G2-D11 was isolated from an antibody phage library obtained from mice immunized with glycopeptides, as previously described (Persson et al. 2016). ScFv sH1 is a codon-optimized (GeneArt) scFv derivative of GOD3-2C4 (Welinder et al. 2011) expressed as previously described (Persson et al. 2016). Bovine serum albumin (BSA) conjugated blood group A antigen was kindly provided by Prof. T. Boren, Umeå. The glycans for glycan array are produced as previously described (Frederiksen et al. 2015).

Glycopeptide and peptide synthesis

All peptides and glycopeptides were prepared by standard Fmoc solid-phase peptide synthesis on an automated Syro I peptide synthesizer (Biotage AB, Sweden), as previously described (Blixt et al. 2010; Blixt and Cló 2013) with some modifications (protocols are presented in [Supplementary data S1](#)). Synthesis was carried out on Tentagel S Rink Amide Resin with a loading density of 0.24 mmol/g (Rapp Polymers GmbH, Germany) with Fmoc for protection of N^α-amino groups; sidechain protecting groups were *tert*-butyl (for Ser, Thr, Glu, Asp), 2,2,4,6,7-pentamethyl-dihydrobenzofuran-5-sulfonyl (Pbf, for Arg), *tert*-butoxycarbonyl (Boc for Lys), and triphenylmethyl (trityl for Asn, Gln, His). For glycopeptide identification, peptides **1–11** and random samples of the trimer library and of the tip synthesis of CD44-peptide were analyzed by electrospray ionization mass spectrometry (ESI-MS) (MSQ Plus Mass Spectrometer, Thermo). Purity (>95%) was evaluated by analytical HPLC (Dionex Ultimate 3000 system) on an analytical C18 column (Phenomenex Gemini NX 110 Å, 5 μ m, C18 particles, 4.60 \times 50 mm) using a linear gradient flow of water-methanol containing 0.1% formic acid (5–100% MeOH in 15 min).

Microarray preparation and analysis

The peptides and the glycopeptides were diluted in print buffer (300 mM phosphate buffer, pH 8.5) to 100 μ M for purified material and 1/20 of crude material. The peptides were printed by robotic pin deposition using a MicroGrid II arrayer (BioRobotics, Genomics Solutions, quilled pins, 250 μ m pitch) onto *N*-hydroxysuccinimide (NHS)-activated glass array slides (SCHOTT NEXTERION® Slide H) (Blixt et al. 2010; Blixt and Cló 2013). The printed slides were placed in a high-humidity chamber for 1 hour. The remaining NHS groups were blocked by immersion in NHS blocking buffer (50 mM ethanolamine in 50 mM borate buffer, pH 9.2) for 30 min just before use. The slides were incubated

with the primary antibody for 1 h with agitation at room temperature (RT) and washed three times with phosphate-buffered saline (PBS). Mouse anti-His antibody (3 µg/mL) was added and incubated for 1 hour with agitation at RT, followed by detection with the secondary antibody, Cy5-conjugated goat anti-mouse IgG (H+L) (Jackson ImmunoResearch Labs, Cat. no 115-175-146) diluted 1:500 in PBS, and incubated for 1 h at RT. All incubation steps were separated by three washing steps with PBS. After the final washing step, the slides were rinsed in water and air dried. The fluorescence signal was measured using a ScanArray 5000 (PerkinElmer) confocal scanner.

Binding kinetics evaluation

OctetRed96 (ForteBio, Menlo Park, CA, USA) was used for BLI studies. Samples and buffers were dispensed into polypropylene 96-well black flat-bottom plates (Greiner Bio-One, Frickenhausen, Germany) at a volume of 200 µL per well, and all measurements were performed at 30°C with agitation at 1000 rpm. Prior to each assay, streptavidin biosensor tips (ForteBio) and Ni-NTA biosensor tips (ForteBio) were prewetted in PBS for at least 10 min followed by equilibration with PBS. The streptavidin biosensor tips were noncovalently loaded with biotinylated IgA1 glycopeptide (Peptide 9, Table I) in PBS with binding kinetics buffer (ForteBio), followed by an additional equilibration step. Association of mAbs in a range of different concentration was performed for 300 s. Finally, the dissociation was monitored with PBS containing binding kinetics buffer for 300 s. The Ni-NTA biosensor tips were loaded with histidine-tagged scFv (6.25 µg/mL) in PBS with binding kinetics buffer (ForteBio), followed by an additional equilibration step. Association of glycopeptides at different concentrations was performed for 60 s. Finally, the dissociation was monitored with PBS containing binding kinetics buffer for 60 s. All measurements were performed in triplicates. The association and dissociation responses were processed with the Octet Software (Version 7.0 and 7.1, ForteBio). Interferometry data was globally fitted to a simple 1:1 Langmuir model calculating the affinities and rate constants.

Immunofluorescence staining of gastric cancer cells

The gastric carcinoma cell line MKN45 was obtained from the Japanese Cancer Research Bank (Tsukuba, Japan) and was stably transfected with the full length human *ST6GALNAC1* gene or the corresponding empty vector pcDNA3.1 as previously described (Marcos et al. 2004). Cells were grown in µ-Chamber 12 well glass slides (IBIDI, Martinsried, Germany) and fixed in cold acetone for 5 min. The mAbs used for immunodetection of Tn-antigen and sialyl-Tn-antigen are described in the Materials section. Samples designed for neuraminidase treatment were incubated with 100 µL of neuraminidase from *C. perfringens* type VI (Sigma-Aldrich, Cat. no N3001) diluted 1:20 in 0.1 M sodium acetate buffer (pH 5) to a final concentration of 0.1 unit/mL. The incubation was carried out for 2 h at 37°C and the reaction was stopped with three washes with cold water. Cells were blocked for 1 h at RT with normal goat serum (DAKO, Cat. no X0907) in PBS with 10% BSA. The primary antibody, 100 µL (2.5 µg/mL) in PBS containing 5% BSA was added and incubated overnight at 4°C and washed with PBS. Anti-His-antibody (R and D Systems, Cat. no MAB050), 100 µL of 2 µg/mL in PBS containing 5% BSA, was added to cells stained with scFv and incubated for 1 h at RT. The slides were washed in PBS before goat anti-mouse IgG-488 (10 µg/mL, Life Technologies, Cat. no A-11029) was added and incubated for 1 h at RT. The slides were washed three times in PBS before and twice after adding DAPI (0.1 µg/mL, 5 min at RT) for nuclear staining. Slides were examined under a Zeiss Imager.Z1 Axio fluorescence microscope (Zeiss, Welwyn Garden City, UK). Images were acquired using a Zeiss Axio cam MRm and the AxioVision Release 4.8.1 software.

IHC of gastric tissue

Formalin fixed paraffin embedded tissue samples from patients with gastric carcinoma were provided by the department of surgical oncology of the University of Siena, Siena, Italy. Ethical permission for the present study was obtained from the local Ethical Committee University of Siena from date 22.06.2015. The FFPE sections were deparaffinised and rehydrated before blocking the endogenous peroxidases with 3% hydrogen peroxide (H₂O₂) in methanol. Tissue sections were further blocked for 30 min at RT with normal rabbit serum (DAKO, Cat. no X0902) diluted 1:5 in PBS containing 10% BSA, followed by incubation with the primary antibodies against Tn-antigen (2.5 µg/mL) overnight at 4°C. After each incubation with antibodies the slides were rinsed in PBS before washing three times in PBS containing 0.02% Tween-20 for 5 min. The anti-His-antibody (R and D Systems, Cat. no MAB050), 2 µg/ml in PBS containing 5% BSA, was added to slides coated with scFv for 30 min and incubated at RT. Rabbit anti-mouse IgG biotin (1:200 dilution, DAKO, Cat. no E0354) was added to all slides for 30 min and incubated at RT. The ABC kit (Vector Labs, Burlingame, CA) for 30 min. Finally, sections were stained by 3,3'-diaminobenzidine tetrahydrochloride (DAB) and counterstained with Gill's hematoxylin solution. The samples were evaluated by a pathologist using a Zeiss Optical Microscope. Immunostaining and the binding pattern of G2-D11, GOD3-2C4 and sH1 were evaluated on the 80 cases of human gastric carcinomas.

ACKNOWLEDGEMENTS

We are grateful to Kasper Kildegaard-Sørensen (University of Copenhagen), Amanda Fritzen (University of Copenhagen) and Lucia Marri (Carlsberg Laboratories) for their technical support. We thank Professor Thomas Borén (Umeå University) for providing blood group A-BSA conjugate and Professor Nicolai Bovin (Russian Academy of Sciences) for providing glycans for glycan array analysis.

FUNDING

This work was supported by the European Union, Seventh Framework Programme, GastricGlycoExplorer (GGE) initial training network [grant number 316929 to OB]; The Danish Research Council [grant number DFF-4005-00285 to OB]; Innovationsfonden in the framework of the EU-ERAsynBio-SynGlycTis project to OB; The EU-IMI 2 Joint Undertaking project EbolaMoDRAD [grant number 115843 to OB]; grants from Mrs. Berta Kamprad's Foundation to CW; FEDER funds through the Operational Programme for Competitiveness Factors-COMPETE [grant number FCOMP-01-0124-FEDER028188 to CR] and National Funds through FCT projects [grant numbers PEst-C/SAU/LA0003/2013, PTDC/BBB-EBI/0567/2014 to CR].

FUNDING

BSA, bovine serum albumin; BLI, bio-layer interferometry; Fmoc, 9-fluorenylmethoxycarbonyl; GalNAc, N-acetylgalactosamine; IHC, immunohistochemistry; NHS, N-hydroxysuccinimide; Ni-NTA, nickel-nitrilotriacetic acid; PBS, phosphate-buffered saline; scFv, single-chain fragment variable, STn, sialyl-Tn; VVL, Vicia villosa lectin.

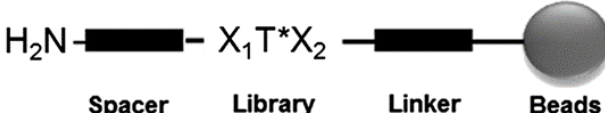
REFERENCES

- Ando H, Matsushita T, Wakitani M, Sato T, Kodama-Nishida S, Shibata K, Shitara K, Ohta S. 2008. Mouse-human chimeric anti-Tn IgG1 induced anti-tumor activity against jurkat cells in vitro and in vivo. *Biol Pharm Bull.* 31(9):1739–1744.
- Avichezer D, Springer GF, Schechter B, Arnon R. 1997. Immunoreactivities of polyclonal and monoclonal anti-T and anti-Tn antibodies with human carcinoma cells, grown in vitro and in a xenograft model. *Int J Cancer.* 72(1):119–127.
- Blixt O, Boos I, Mandel U. 2012a. Glycan microarray analysis of tumor-associated antibodies. In: Kosma P, Müller-Loennies S, editors. *Anticarbhydrate Antibodies: From Molecular Basis to Clinical Application*. Vienna: Springer Vienna. p.283–306.
- Blixt O, Bueti D, Burford B, Allen D, Julien S, Hollingsworth M, Gammerman A, Fentiman I, Taylor-Papadimitriou J, Burchell JM. 2011. Autoantibodies to aberrantly glycosylated MUC1 in early stage breast cancer are associated with a better prognosis. *Breast Cancer Res.* 13(2): R25–R25.
- Blixt O, Cló E. 2013. Synthesis of O-glycopeptides and construction of glycopeptide microarrays. In: Jensen JK, Tofteng Shelton P, Pedersen LS, editors. *Peptide Synthesis and Applications*. Totowa, NJ: Humana Press. p.201–214.
- Blixt O, Cló E, Nudelman AS, Sørensen KK, Clausen T, Wandall HH, Livingston PO, Clausen H, Jensen KJ. 2010. A high-throughput O-glycopeptide discovery platform for seromic profiling. *J Proteome Res.* 9(10):5250–5261.
- Blixt O, Lavrova OI, Mazurov DV, Cló E, Krac̃un SK, Bovin NV, Filatov AV. 2012b. Analysis of Tn antigenicity with a panel of new IgM and IgG1 monoclonal antibodies raised against leukemic cells. *Glycobiology.* 22(4):529–542.
- Brooks CL, Schietinger A, Borisova SN, Kufer P, Okon M, Hiram T, MacKenzie CR, Wang L-X, Schreiber H, Evans SV. 2010. Antibody recognition of a unique tumor-specific glycopeptide antigen. *Proc Natl Acad Sci U S A.* 107(22):10056–10061.
- Conze T, Carvalho AS, Landegren U, Almeida R, Reis CA, David L, Söderberg O. 2009. MUC2 mucin is a major carrier of the cancer-associated sialyl-Tn antigen in intestinal metaplasia and gastric carcinomas. *Glycobiology.* 20(2):199–206.
- Desai PR. 2000. Immunoreactive T and Tn antigens in malignancy: role in carcinoma diagnosis, prognosis, and immunotherapy. *Transfus Med Rev.* 14(4):312–325.
- Ferreira B, Marcos NT, David L, Nakayama J, Reis CA. 2006. Terminal α 1,4-linked N-acetylglucosamine in helicobacter pylori-associated intestinal metaplasia of the human stomach and gastric carcinoma cell lines. *J Histochem Cytochem.* 54(5):585–591.
- Frederiksen RF, Yoshimura Y, Storgaard BG, Paspaliari DK, Petersen BO, Chen K, Larsen T, Duus JØ, Ingmer H, Bovin NV, et al. 2015. A diverse range of bacterial and eukaryotic chitinases hydrolyzes the LacNAc (Gal β 1-4GlcNAc) and LacdiNAc (GalNAc β 1-4GlcNAc) motifs found on vertebrate and insect cells. *J Biol Chem.* 290(9):5354–5366.
- Gill DJ, Chia J, Senewiratne J, Bard F. 2010. Regulation of O-glycosylation through Golgi-to-ER relocation of initiation enzymes. *J Cell Biol.* 189(5): 843–858.
- Hamada S, Furumoto H, Kamada M, Hirao T, Aono T. 1993. High expression rate of Tn antigen in metastatic lesions of uterine cervical cancers. *Cancer Lett.* 74(3):167–173.
- Ju T, Otto VI, Cummings RD. 2011. The Tn antigen—structural simplicity and biological complexity. *Angew Chem Int Ed.* 50(8):1770–1791.

- Li Q, Anver MR, Butcher DO, Gildersleeve JC. 2009. Resolving conflicting data on expression of the Tn antigen and implications for clinical trials with cancer vaccines. *Mol Cancer Ther.* 8(4):971–979.
- Madariaga D, Martínez-Sáez N, Somovilla VJ, Coelho H, Valero-González J, Castro-López J, Asensio JL, Jiménez-Barbero J, Busto JH, Avenzoza A, et al. 2015. Detection of tumor-associated glycopeptides by lectins: the peptide context modulates carbohydrate recognition. *ACS Chem Biol.* 10(3):747–756.
- Madariaga D, Martínez-Sáez N, Somovilla VJ, García-García L, Berbis MÁ, Valero-González J, Martín-Santamaría S, Hurtado-Guerrero R, Asensio JL, Jiménez-Barbero J, et al. 2014. Serine versus threonine glycosylation with α -O-GalNAc: unexpected selectivity in their molecular recognition with lectins. *Chemistry.* 20(39):12616–12627.
- Marcos NT, Pinho S, Grandela C, Cruz A, Samyn-Petit B, Harduin-Lepers A, Almeida R, Silva F, Morais V, Costa J, et al. 2004. Role of the human ST6GalNAc-I and ST6GalNAc-II in the synthesis of the cancer-associated sialyl-Tn antigen. *Cancer Res.* 64(19):7050–7057.
- Mazal D, Lo-Man R, Bay S, Pritsch O, Dériaud E, Ganneau C, Medeiros A, Ubillos L, Obal G, Berois N, et al. 2013. Monoclonal antibodies toward different Tn-amino acid backbones display distinct recognition patterns on human cancer cells. Implications for effective immuno-targeting of cancer. *Cancer Immunol Immunother.* 62(6):1107–1122.
- Nakada H, Inoue M, Tanaka N, Numata Y, Kitagawa H, Fukui S, Yamashina I. 1991. Expression of the Tn antigen on T-lymphoid cell line Jurkat. *Biochem Biophys Res Commun.* 179(2):762–767.
- Numata Y, Nakada H, Fukui S, Kitagawa H, Ozaki K, Inoue M, Kawasaki T, Funakoshi I, Yamashina I. 1990. A monoclonal antibody directed to Tn antigen. *Biochem Biophys Res Commun.* 170(3):981–985.
- Ohshio G, Imamura T, Imamura M, Yamabe H, Sakahara H, Nakada H, Yamashina I. 1995. Distribution of Tn antigen recognized by an anti-Tn monoclonal antibody (MLS128) in normal and malignant tissues of the digestive tract. *J Cancer Res Clin Oncol.* 121(4):247–252.
- Oshikiri T, Miyamoto M, Morita T, Fujita M, Miyasaka Y, Senmaru N, Yamada H, Takahashi T, Horita S, Kondo S. 2006. Tumor-associated antigen recognized by the 22-1-1 monoclonal antibody encourages colorectal cancer progression under the scanty CD8+ T cells. *Clin Cancer Res.* 12(2):411–416.
- Osinaga E, Bay S, Tello D, Babino A, Pritsch O, Assemat K, Cantacuzene D, Nakada H, Alzari P. 2000. Analysis of the fine specificity of Tn-binding proteins using synthetic glycopeptide epitopes and a biosensor based on surface plasmon resonance spectroscopy. *FEBS Lett.* 469(1):24–28.
- Pancino GF, Osinaga E, Vorauer W, Kakouche A, Mistro D, Charpin C, Roseto A. 1990. Production of a monoclonal antibody as immunohistochemical marker on paraffin embedded tissues using a new immunization method. *Hybridoma.* 9(4):389–395.
- Persson N, Jansson B, Stühr-Hansen N, Kovács A, Welinder C, Danielsson L, Blixt O. 2016. A combinatory antibody-antigen microarray assay for high-content screening of single-chain fragment variable clones from recombinant libraries. *PLOS ONE.* 11(12):e0168761.
- Pinho S, Marcos NT, Ferreira B, Carvalho AS, Oliveira MJ, Santos-Silva F, Harduin-Lepers A, Reis CA. 2007. Biological significance of cancer-associated sialyl-Tn antigen: Modulation of malignant phenotype in gastric carcinoma cells. *Cancer Lett.* 249(2):157–170.
- Pinho SS, Reis CA. 2015. Glycosylation in cancer: Mechanisms and clinical implications. *Nat Rev Cancer.* 15(9):540–555.
- Posey AD Jr, Schwab Robert D, Boesteanu Alina C, Steentoft C, Mandel U, Engels B, Stone Jennifer D, Madsen Thomas D, Schreiber K, Haines Kathleen M, et al. 2016. Engineered CAR T cells targeting the cancer-associated Tn-glycoform of the membrane mucin MUC1 control adenocarcinoma. *Immunity.* 44(6):1444–1454.

- Reis CA, Sørensen T, Mandel U, David L, Mirgorodskaya E, Roepstorff P, Kihlberg J, Stig Hansen J-E, Clausen H. 1998. Development and characterization of an antibody directed to an α -N-acetyl-D-galactosamine glycosylated MUC2 peptide. *Glycoconj J*. 15(1):51–62.
- Sakai K, Yuasa N, Tsukamoto K, Takasaki-Matsumoto A, Yajima Y, Sato R, Kawakami H, Mizuno M, Takayanagi A, Shimizu N, et al. 2010. Isolation and characterization of antibodies against three consecutive Tn antigen clusters from a phage library displaying human single-chain variable fragments. *J Biochem*. 147(6):809–817.
- Springer FG. 1997. Immunoreactive T and Tn epitopes in cancer diagnosis, prognosis, and immunotherapy. *J Mol Med*. 75(8):594–602.
- Takahashi HK, Metoki R, Hakomori S-I. 1988. Immunoglobulin G3 monoclonal antibody directed to Tn antigen (tumor-associated α -N-acetylgalactosaminyl epitope) that does not cross-react with blood group A antigen. *Cancer Res*. 48(15):4361–4367.
- Tomana M, Novak J, Julian BA, Matousovic K, Konecny K, Mestecky J. 1999. Circulating immune complexes in IgA nephropathy consist of IgA1 with galactose-deficient hinge region and antiglycan antibodies. *J Clin Invest*. 104(1):73–81.
- Welinder C, Baldetorp B, Blixt O, Grabau D, Jansson B. 2013. Primary breast cancer tumours contain high amounts of IgA1 immunoglobulin: an immunohistochemical analysis of a possible carrier of the tumour-associated Tn antigen. *PLoS ONE*. 8(4):e61749.
- Welinder C, Baldetorp B, Borrebaeck C, Fredlund B-M, Jansson B. 2011. A new murine IgG1 anti-Tn monoclonal antibody with in vivo anti-tumor activity. *Glycobiology*. 21(8):1097–1107.
- Wu AM. 2004. Polyvalency of Tn (GalNAc α 1 \rightarrow Ser/Thr) glycotopes as a critical factor for Vicia villosa B4 and glycoprotein interactions. *FEBS Lett*. 562(1–3):51–58.
- Yu L-G. 2007. The oncofetal Thomsen–Friedenreich carbohydrate antigen in cancer progression. *Glycoconj J*. 24(8):411–420.
- Yuasa N, Ogawa H, Koizumi T, Tsukamoto K, Matsumoto-Takasaki A, Asanuma H, Nakada H, Fujita-Yamaguchi Y. 2012. Construction and expression of anti-Tn-antigen-specific single-chain antibody genes from hybridoma producing MLS128 monoclonal antibody. *J Biochem*. 151(4):371–381.
- Zhang S, Zhang HS, Reuter VE, Slovin SF, Scher HI, Livingston PO. 1998. Expression of potential target antigens for immunotherapy on primary and metastatic prostate cancers. *Clin Cancer Res*. 4(2):295–302.

FIGURES



H₂N
—
[Spacer]
—
X₁T*X₂
—
[Linker]
—
[Beads]

Groups	Sequence (GalNAc*)	Amino acid (X)	No of combinations
Group 1	X ₁ T*T*	X ₁ = C, D, E, H, I, K, L, M, N, P, Q, R, S, T, V, W or Y	17
Group 2	T*T*X ₂	X ₂ = A, D, E, F, G, I, K, L, M, N, P, Q, S, T, V, W or Y	17
Group 3	X ₁ T*S*	X ₁ = D, E, H, I, K, L, M, N, Q, R, S, T, V, W or Y	15
Group 4	S*T*X ₂	X ₂ = D, E, H, K, R or T	6
Group 5a	X ₁ T*X ₂	X ₁ =F, G, I, L, M, P, V, W or Y X ₂ = A, C, D, E, F, G, H, I, K, L, M, N, P, Q, R, S, T, V, W or Y	145
Group 5b	X ₁ T*X ₂	X ₁ = D, E, H, K, L, N, Q, R, S or T X ₂ = A, C, D, E, F, G, H, I, K, L, M, N, P, Q, R, S, T, V, W or Y	186

Figure 1 - Trimer glycopeptide library. General structure of the trimer glycopeptide library with three amino acids (X₁X₂X₃) having GalNAc at different positions. Peptides were synthesized on beads and cleaved off, before being printed on the array. The library was divided into five different groups based on the position of GalNAc (*). The amino acids flanking the GalNAc are presented for each group. The number of specific combinations of amino acids tested is specified under "No of combinations."

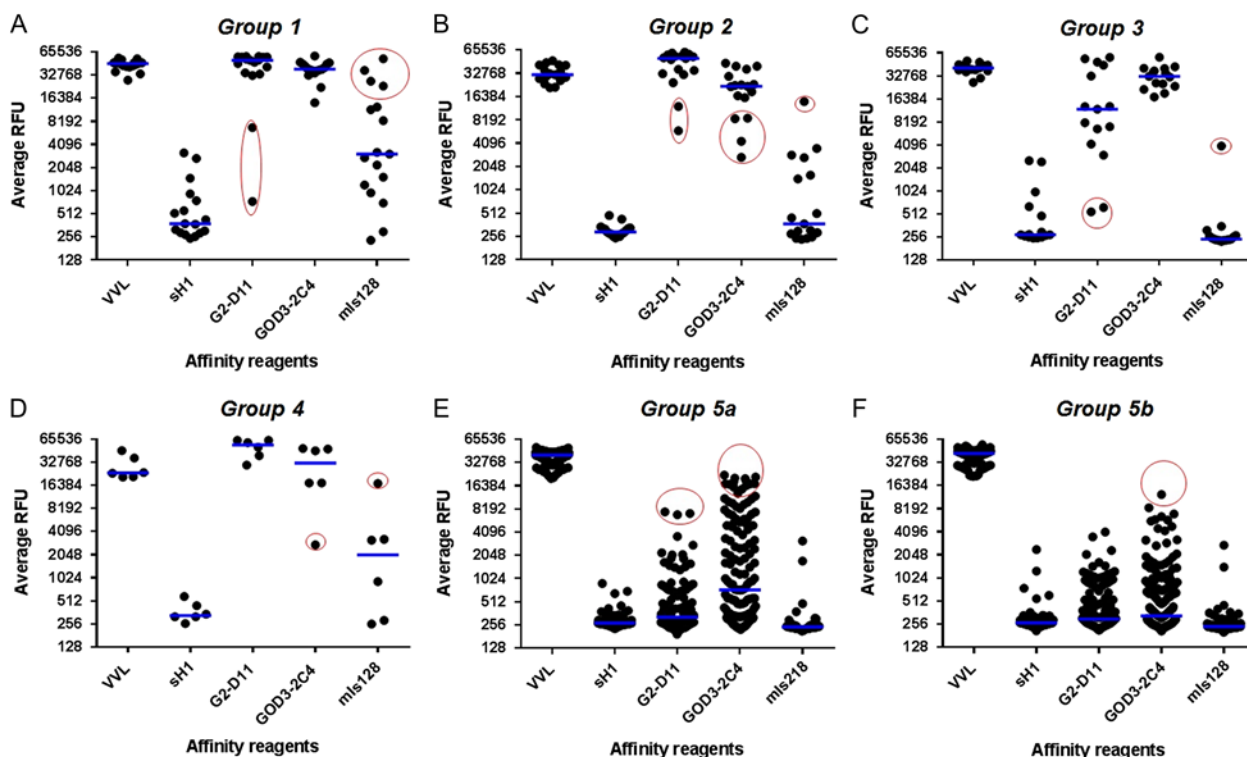


Fig. 2. Specificity of VVL and antibodies on large trimer amino acid glycopeptide library, printed on microarray slides. The library was divided into five groups according to the position of glycosylated (GalNAc) serine (S*) and threonine (T*) in relation to other amino acids (X) as described in Figure 1. VVL, scFv sH1 and G2-D11, mouse monoclonal GOD3-2C4 and MLS128 antibodies were tested in all combinations. Each dot represents a unique sub-library member. Median signals for each group of combinations are marked with a blue line and a red circle is highlighting amino acids (X) affecting binding of the reagents. (A) Group 1 (XT*T*). (B) Group 2 (T*T*X). (C) Group 3 (XT*S*). (D) Group 4 (S*T*X). (E) Group 5a (GT*X₃, PT*X₃, WT*X₃, IT*X₃, LT*X₃, MT*X₃, FT*X₃, YT*X₃ and VT*X₃), where G2-D11 bound to FT*R, WT*K, YT*W and YT*A, and GOD3-2C4 bound to VT*N, VT*M, VT*W, WT*C, WT*D, WT*E, WT*I, WT*M, WT*N, YT*F, YT*M and YT*R. (F) Group 5b (RT*X₃, HT*X₃, KT*X₃, DT*X₃, ET*X₃, ST*X₃, TT*X₃, NT*X₃ and QT*X₃), where GOD3-2C4 bound to HT*R. This figure is available in black and white in print and in colour at Glycobiology online.

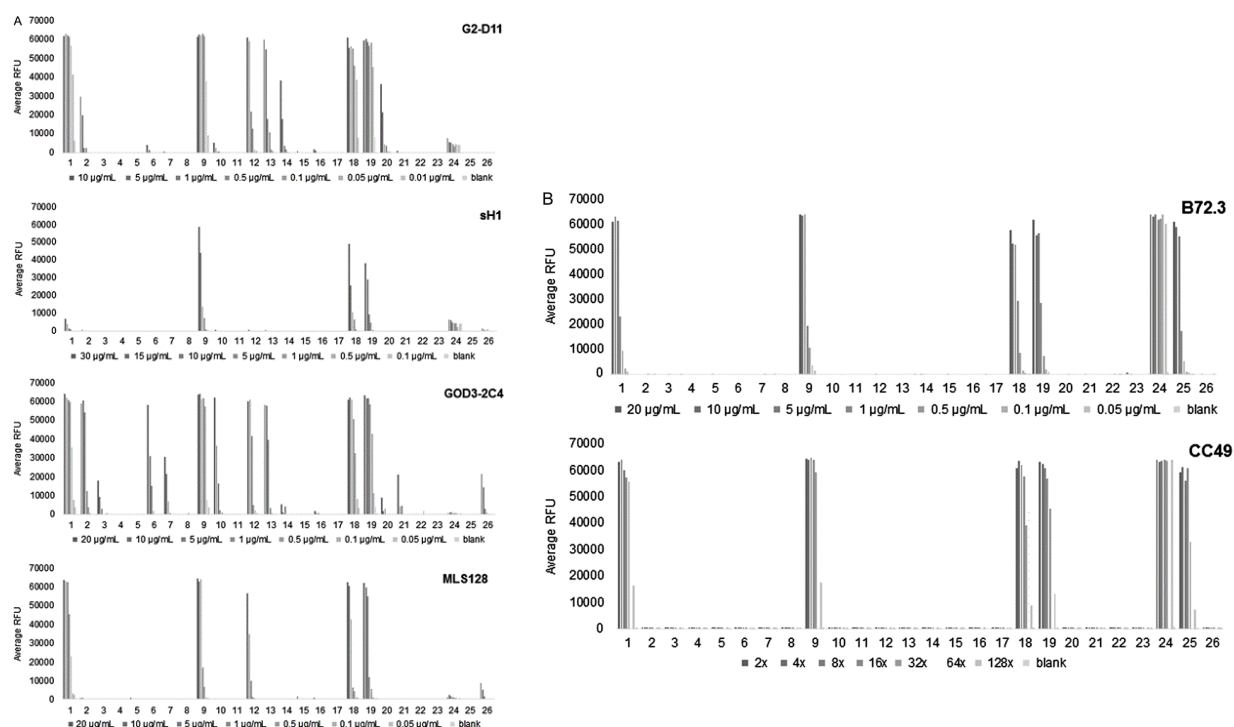


Fig. 3. (A) Specificity evaluation of Tn-binding antibodies on glycopeptide microarray. Glycopeptides according to Table I were printed on a microarray chip. ScFv G2-D11 was titrated from 10 µg/mL in a series of 5, 1, 0.5, 0.1, 0.05 and 0.01 µg/mL, and scFv sH1 from 30 µg/mL in a series of 15, 10, 5, 1, 0.5 and 0.1 µg/mL, GOD3-2C4 and MLS128 were titrated from 20 µg/mL in a series of 10, 5, 1, 0.5, 0.1 and 0.05 µg/mL. (B) Specificity evaluation of STn binding antibodies on glycopeptide microarray. Glycopeptides according to Table I were printed on a microarray chip. B72.3 was titrated from 20 µg/mL in a series of 10, 5, 1, 0.5, 0.1, and 0.05 µg/mL. The supernatant containing CC49 was diluted in a 2-fold series.

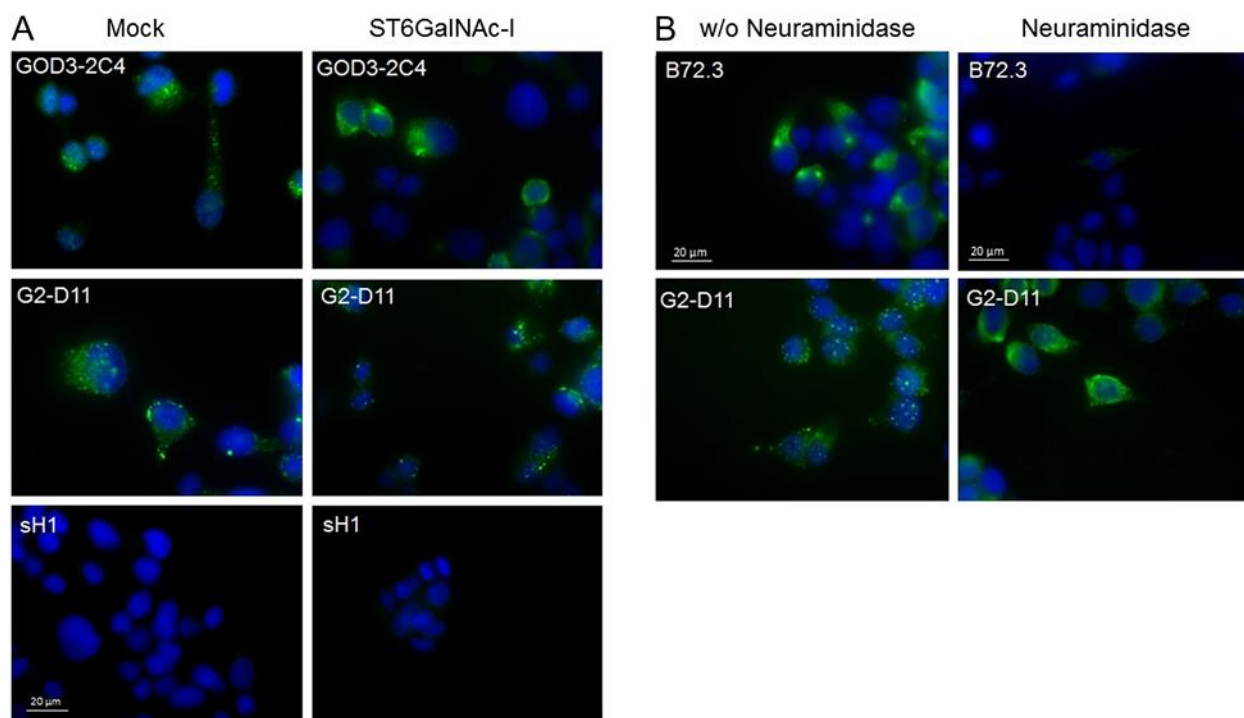


Fig. 4. Immunofluorescence staining of mock and ST6GALNAC₁ transfected MKN45 cells. (A) Staining of mock MKN45 and ST6GALNAC₁ transfected MKN45 with GOD3-2C₄, G2-D11 and sH1. To be able to see the binding pattern of GOD3-2C₄, a longer exposure time was required compared to G2-D11 and sH1. (B) ST6GALNAC₁ transfected MKN45 cells with or without neuraminidase treatment and stained with sialyl-Tn-antigen binding antibody B72.3 and Tn-antigen binding scFv G2-D11. A 630x magnification was used with a shorter exposure time for B72.3 than for G2-D11 as the staining with B72.3 at the same exposure time was over expressed. This figure is available in black and white in print and in colour at Glycobiology online.

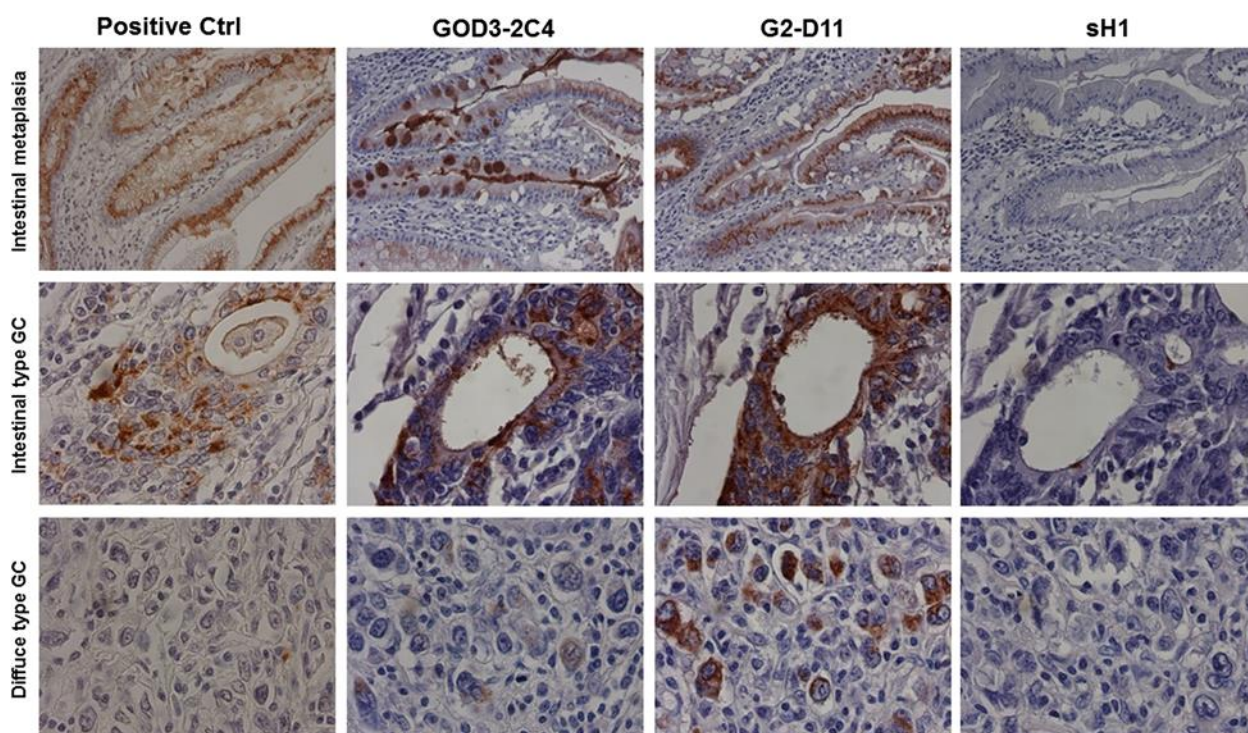


Fig. 5. IHC comparison between different antibodies on gastric tissues. Anti-Tn-antigen antibody GOD3-2C4, anti-Tn-antigen scFv antibodies G2-D11 and sH1 and positive antibody control (1E3) staining of intestinal metaplasia, diffuse type gastric cancer and intestinal type gastric cancer. A 200x magnification was used for intestinal metaplasia and 630x for the remaining pictures. This figure is available in black and white in print and in colour at Glycobiology online.

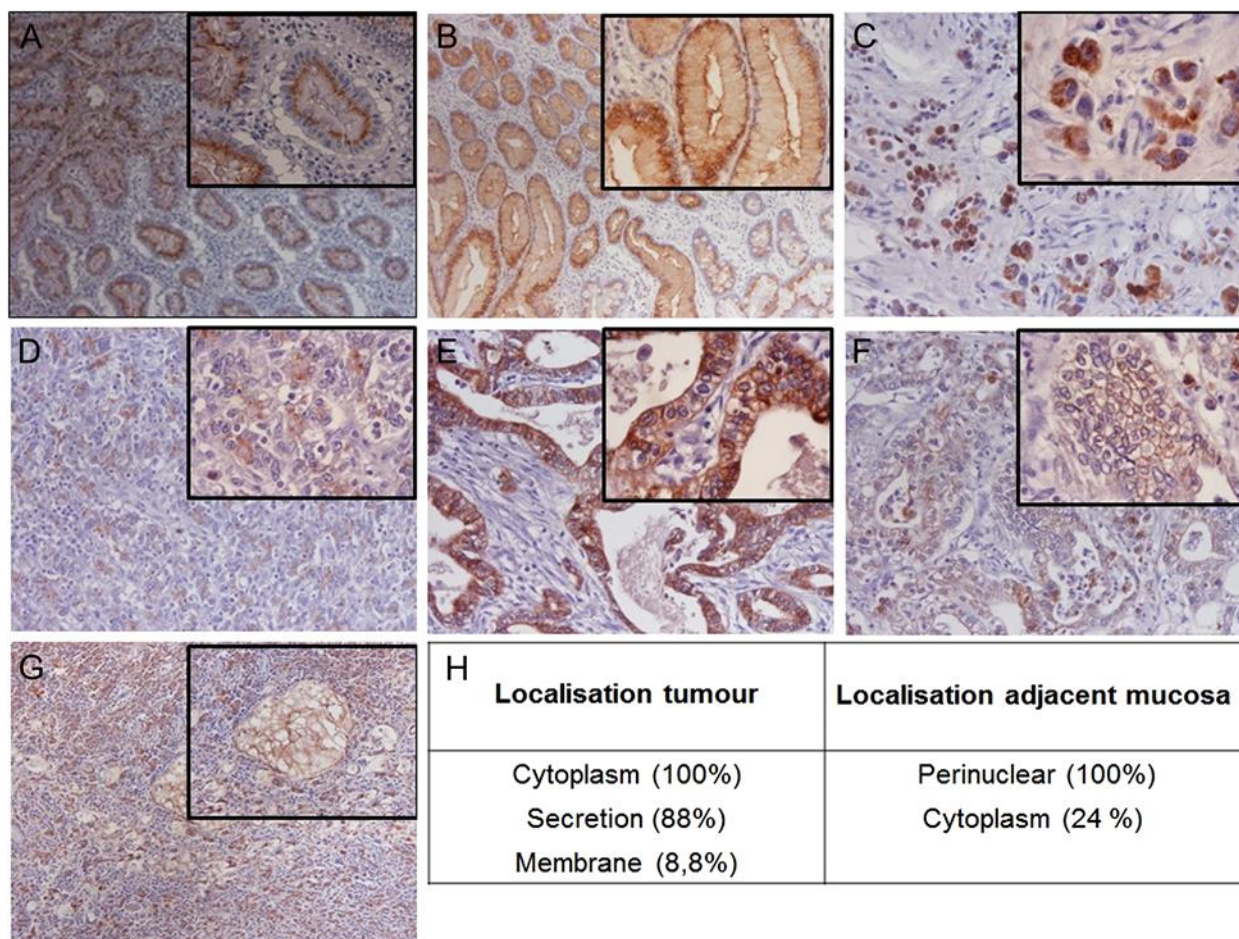


Fig. 6. IHC staining of gastric tissue, using scFv G2-D11. (A, B) Perinuclear staining of normal adjacent mucosa. (C, D) Cytoplasmic staining of tumor cells. (E, F) Cytoplasmic and membrane staining of tumor cells. (G) Staining of mucin lakes within the carcinoma. A 200x magnification was used for the large picture and 630x magnification was used for the inserted picture with the exception of picture C with 100x for larger picture and 200x for the inserted picture. (H) Summary of localization of the G2-D11 staining on 80 cases of gastric carcinoma. This figure is available in black and white in print and in colour at Glycobiology online.

TABLES

Table I. Glycopeptide sequences of short tetramer and 20-mer peptides of MUC1, IgA1 and CD44 on microarray chip

Peptide number on array	Peptide sequence	Peptide number on array	Peptide sequence
1	S*T*GK	14	EEDKDHPPT*S*TLTSSNRNDV
2	T*S*GK	15	EEDKDHPPT*STLTSSNRNDV
3	S*TGK	16	EEDKDHPPT*STLTSSNRNDV
4	ST*GK	17	EEDKDHPPT*STLTSSNRNDV
5	T*SGK	18	GYRQTPKEDSHS*T*GTAAAS
6	TS*GK	19	GYRQTPKEDSHS*T*GTAAAS
7	S*GK	20	GYRQTPKEDSHS*T*GTAAAS
8	T*GK	21	GYRQTPKEDSHS*TTGTAAAS
9	VPSTPPTSPS*T*PPTSPSA	22	GYRQTPKEDSHS*TTGTAAAS
10	VPSTPPTSPS*TPPTSPSA	23	GYRQTPKEDSHS*TTGTAAAS
11	VPSTPPTSPS*TPPTSPSA	24	VTSAPDT*RPAGS*T*APPAGH("STn") [#]
12	EEDKDHPPT*T*S*TLTSSNRNDV	25	APGSTAPPAHGVTS*APDT*RP("STn") [#]
13	EEDKDHPPT*T*STLTSSNRNDV	26	Blood group A-BSA conjugate

*: GalNAc; "": STn; #: Blixt et al. (2011).

Table II. Analysis of binding kinetics of G2-D11, sH1 and GOD3-2C4 to peptide 9

Antibody	Immobilized entity	K_{on} (1/Ms)	K_{off} (1/s)	K_D (M)
G2-D11	Antigen	8.70E+04	2.51E-03	2.34E-08
GOD3-2C4	Antigen	1.78E+05	3.08E-03	1.73E-08
sH1	Antigen	*	*	*
G2-D11	scFv	1.35E+05	1.78E-03	1.33E-08
sH1	scFv	*	*	*

Measured with BLI using antigen or scFv immobilized on sensor tips (sensors in Supplementary data Figure S2). *No conclusions could be drawn from the analysis due to very low signal and bad fit to theoretical curve of the Langmuir model.

Table III. IHC evaluation of G2-D11 on gastric carcinoma ($n = 80$)

Group	Tumor staining (%)	Intensity	n (%)	Percentage in group
High	>75	+	1 (1.3)	58.7
	>75	++	14 (17.7)	
	>75	+++	10 (11.4)	
	50-75	+	4 (5.1)	
	50-75	++	17 (20.3)	
	50-75	+++	1 (1.3)	
Medium	25-50	+	7 (8.9)	23.8
	25-50	++	12 (15.2)	
	25-50	+++	0 (0)	
Low	<25	+	11 (13.9)	17.5
	<25	++	3 (3.8)	
	<25	+++	0 (0)	

Data on tumor staining and intensity of G2-D11 staining in tumor area. The cohort is divided into groups: high, medium and low, depending on the percentage of tumor staining.